

A concept of heterogeneous numerical model of concrete for GPR simulations

J. Lachowicz, M. Rucka

Faculty of Civil and Environmental Engineering
Gdańsk University of Technology
Gdańsk, Poland
jaclacho@pg.gda.pl, mrucka@pg.gda.pl

Abstract—The Ground Penetrating Radar (GPR) method, which is increasingly being used in the non-destructive diagnostics of reinforced concrete structures, often needs more accurate interpretation tools for analysis of experimental data. Recently, there has been growing interest in developing of various numerical models for exhaustive understanding of GPR data. This paper presents the concept of a heterogeneous numerical model of concrete, in which individual components of concrete are separate materials and their location in the model is pseudo-random. The numerical model was validated with the Complex Refractive Index Model (CRIM). In addition, experimental surveys were conducted on a reinforced concrete footbridge with high saturation of water. Experimental radargrams were compared with numerical GPR maps, calculated using both homogeneous and heterogeneous models of concrete.

Keywords—FDTD modelling; GPR simulations; concrete; heterogeneous numerical model

I. INTRODUCTION

The Ground Penetrating Radar (GPR) method is increasingly being used in the non-destructive diagnostics of reinforced concrete structures. It is very efficient technique but often it requires more accurate interpretation tools for exhaustive analysis of in-situ surveys. Numerical modelling of electromagnetic field propagation is an invaluable aid in the interpretation of GPR data. It enables understanding the origin of the individual reflections and diffractions in GPR maps. It also allows to gain the necessary experience in analysing radargrams. In traditional numerical modelling dedicated to support the GPR diagnostics, materials are treated as homogenous. Nowadays there is a growing interest in developing of more precise, heterogeneous models of a medium in which GPR field propagates. A heterogeneous mixing model of soil was proposed by Peplinski et al. [1]. The material model was successfully used for numerical modelling of GPR mine detection in the ground with regard of the rough surface, surface water and antenna model [2]. In the case of concrete, which is also a heterogeneous material, research is directed to measurements of electrical properties [4] and identification of parameters of dielectric models of heterogeneous mixtures.

The aim of the study is to develop a numerical model of heterogeneous and porous concrete that will be closer to reality than the homogeneous model. In the proposed model, individual components of concrete are separate materials and their location in the model is pseudo-random. The numerical model was validated with the Complex Refractive Index Model (CRIM). An application of the model was presented on the example of diagnostics of a reinforced concrete footbridge with high saturation of water. Experimental radargrams were compared with numerical GPR maps, calculated using both the homogeneous model and the proposed heterogeneous model of concrete.

II. MODEL DESCRIPTION

The numerical model is based on the Finite-Difference Time-Domain (FDTD) method, featuring a representation of a material by creation of a matrix of electrical parameters (the permittivity, permeability, magnetic and electric conductivity) at nodes of Yee cells. The equation describing the effective permittivity ϵ_e is defined as [5]:

$$\epsilon_e = \epsilon + \frac{\sigma}{i\omega} = \epsilon'_e - i\epsilon''_e \quad (1)$$

where ϵ'_e is the real part of the permittivity, ϵ''_e is the imaginary part of the permittivity, σ is the conductivity, ω is the angular frequency and i stands for the complex imaginary number.

In the case of a homogeneous material, each Yee cell has assigned the same electrical properties. For non-destructive testing purposes, concrete is often modelled as a homogeneous material (e.g. [6]), and for most cases, it is a sufficient simplification. However, in fact concrete is composed of coarse and fine aggregate, cement, water and air as well as secondary dopants. In other words, concrete is a mixture of different phases. Dry concrete composed only of the gaseous and solid phases is not a dispersive material, i.e. it is not dependent on the frequency [5]. The dispersion in concrete is mainly caused by the existence of water in concrete pores. Therefore, the modelling of concrete is possible using dispersion models such as the Debye model, as shown in [4]. The simplest model which has been successfully used to estimate the relative effective permittivity for heterogeneous materials like rocks,

soils or concrete is the Complex Refractive Index Model (CRIM) [5]:

$$\sqrt{\epsilon_r} = (1 - \Phi)\sqrt{\epsilon_m} + (1 - S_w)\Phi\sqrt{\epsilon_a} + \Phi S_w\sqrt{\epsilon_{sw}} \quad (2)$$

where Φ is the porosity of concrete, S_w is the degree of pores saturation, ϵ_r is the relative effective permittivity of concrete, ϵ_m is the relative permittivity of the solid phase (matrix), ϵ_a is the relative permittivity of the gaseous phase (air) and ϵ_{sw} is the relative permittivity of the liquid phase (water).

In this paper we propose a numerical model, in which the distribution of individual components of concrete is pseudo-random. A script wrote in Python generates a random position for the individual component of concrete, taking into account the percentage distribution of fractions and their dimensions. Any grading curve of aggregate composed of a fraction from 1 mm to 32 mm can be applied (see Fig. 1a). For each fraction different electrical properties can be assigned. Previous research shows that salinity has a major impact on the electrical parameters of water, which also affects the parameters of concrete [3]. Therefore, the proposed model can also take into account the content of chloride by changing the electrical properties of water, or by adding another fraction. Fig. 1a shows a selected grading curve and concrete content. The visualisation of distribution of individual components of concrete in the proposed model is given in Fig. 1b.

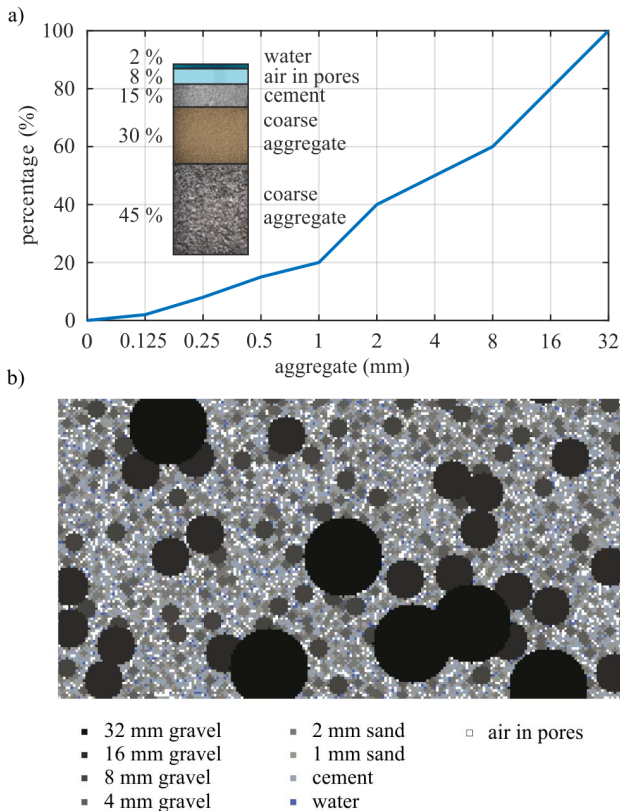


Fig. 1. a) concrete content and grading curve of aggregate b) visualisation of distribution of individual components of concrete in the proposed heterogeneous model

III. MODEL VERIFICATION

In order to investigate the behaviour of the heterogeneous model of concrete, GPR simulations were performed using gprMax [7], for concrete slabs with different degree of saturation examined experimentally by Laurens et al. [5]. The geometry of concrete samples was: 25 cm \times 25 cm \times 7 cm. In addition, a steel plate was inserted on the bottom of the sample in order to increase the amplitude of the reflected signal. Different degree of concrete saturation, varied from 0 % to 100% with an interval of 10%, was considered. The porosity of concrete was assumed as 14% after [5]. The geometry of the model for saturation of 60% is shown in Fig. 2.

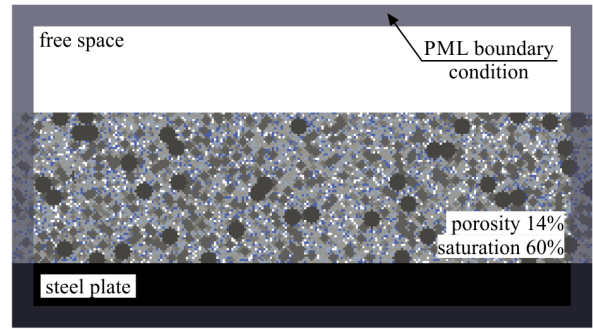


Fig. 2. Numerical model of concrete sample for saturation of 60%

The excitation signal was assumed as a Ricker function with a central frequency of 1.3 GHz. The distance between the dipole and the receiver has been set as $dx = 0.001$ mm (i.e. the distance between the Yee cell nodes). Calculation parameters used for the numerical model are given in Table 1.

TABLE I. PARAMETERS FOR NUMERICAL MODEL

| Parameter | Numerical after [5] | Numerical validated | Numerical with conductivity |
|--|---------------------|---------------------|-----------------------------|
| Permittivity of the gaseous phase ϵ_a | 1 | 1 | 1 |
| Permittivity of the solid phase ϵ_m | 4 | 3,64 | 3,62 |
| Permittivity of the liquid phase ϵ_{sw} | 74,5 | 37,54 | 39,64 |
| Conductivity σ | - | - | 3,25 S/m |

In GPR simulations, 25 A-scans were calculated along the concrete sample. The two-way travel time was identified between the first negative peak of the direct wave and the first positive peak of the reflected signal (see Fig. 3).

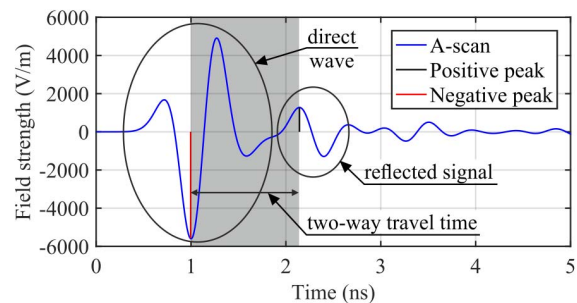


Fig. 3. Typical A-scan for the numerical model

On the basis of the two-way travel time, the velocity was identified, and then the dielectric constant value was calculated as an average of 25 A-scans. The average values of the permittivity for different degree of saturation are compared in Fig. 4 with results of experimental studies and results of CRIM simulations [5].

It has been revealed that the results do not coincide with the experimental ones. It turned out that the calculated effective permittivity is close to the weighted average of permittivity and the volume.

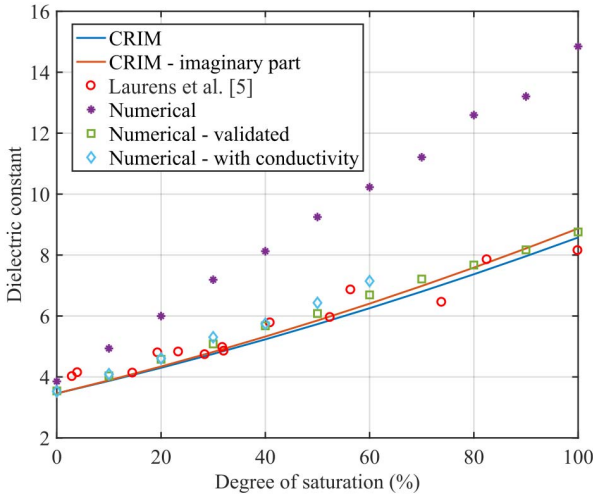


Fig. 4. Effect of degree of saturation on dielectric constant

In order to find a good agreement between the numerical and experiment results, a validation of the numerical model was performed and a nonlinear fitting of parameters was conducted. The permittivity of two phases (solid and liquid) was fitted to the nonlinear CRIM. In this manner, the substitute water permittivity $\epsilon_{sw} = 37.54$ and the substitute permittivity of the solid phase $\epsilon_m = 3.64$ were obtained. The results of numerical simulations using the validated model are plotted in Fig. 4.

Afterwards, in the CRIM, the imaginary part of the water permittivity was included, which is responsible for the losses within the medium. The results for this model are included in Fig. 4. Due to the use of the substitute permittivity in the Debye model, the dispersion for water cannot be applied. Therefore the dispersive properties of the water were assumed as the conductivity according to the formula [8]:

$$\sigma = \omega \cdot \epsilon'' \quad (3)$$

Again the nonlinear fitting was carried out providing the following parameters: $\epsilon_{sw} = 39.64$, $\sigma = 3.25 \text{ S / m}$ and $\epsilon_m = 3.62$. Results for the validated model with conductivity are printed in Fig. 4. A reliable numerical solutions with the water conductivity were obtained only up to 60 % of saturation because with higher saturation the amplitude of the reflected signal was unnoticeable. The difference between A-scans for the validated model with the conductivity of the water and

without the conductivity is presented in Fig. 5. It can be seen that the reflected signal for the model with the conductivity is much weaker than in the model without the conductivity.

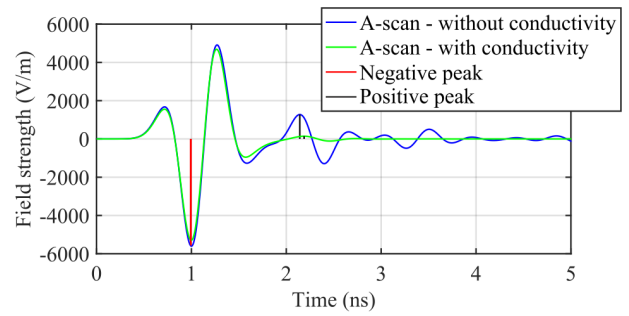


Fig. 5. Selected A-scans for the model with and without conductivity for the concrete sample with 50 % of saturation

IV. APPLICATION OF THE MODEL

The above-described heterogeneous model of concrete is intended for GPR simulations of saturated concrete structures or concrete structures that are in the early stages of hydration. The example of a radargram acquired for a structure turning up in such conditions is given in Fig. 6. Experimental research was conducted on a footbridge shortly after building and after rainy weather. The tests were performed with a GPR antenna with a centre frequency equal to 2 GHz. Fig. 6 shows a segment of a GPR map along the footbridge. The deck is a 50 cm height plate reinforced by stirrups of 12 mm diameter with 125 mm of spacing. On the GPR map only reflections from the upper transverse reinforcement can be seen. Bottom reinforcement and the bottom of the deck are not detectable, most probably due to the presence of a significant quantity of water in the concrete pores.

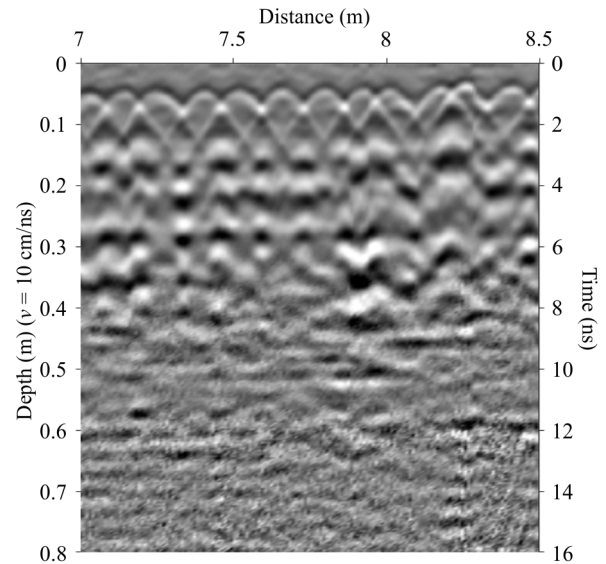


Fig. 6. Experimental radargram for a footbridge

Two numerical models of the footbridge were created: the first in which concrete is the homogeneous material, and the second with heterogeneous distribution of fractions assuming

that the porosity of concrete was 15% and the saturation was equal to 50%. Parameters and the distribution of fractions were chosen so that the effective permittivity of concrete was equal to 9. Numerical 2D models with the outer dimensions of 160 cm x 60 cm discretized using square cells of dimensions $dx = dy = 1$ mm are presented in Fig. 7. The distance between the source and the receiver was assumed as 6 cm like the offset of the transmitter and receiver in the antenna used for experimental studies. The signal was applied as a Ricker function with a central frequency of 2 GHz.

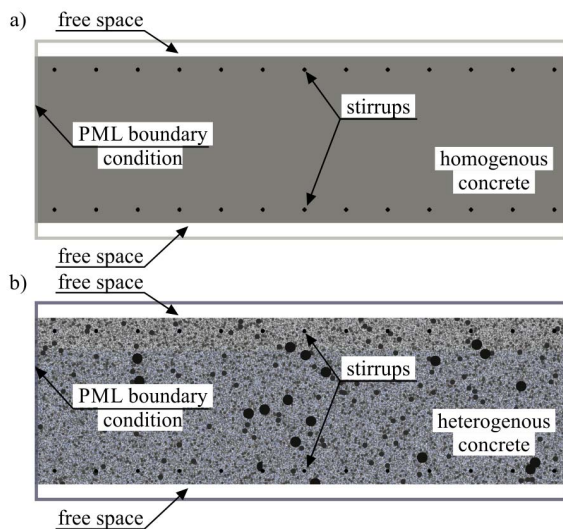


Fig. 7. Numerical models of a footbridge for a) homogenous and b) heterogeneous models of concrete

Calculated GPR map are shown in Fig. 8. In the case of the homogeneous model, reflections from the upper and lower bars and the lower edge are clearly visible. In the case of the heterogeneous model, strong and clear reflections can be noticed only for the upper bars as in experimental studies. High water content caused that neither lower bars nor the bottom edge were detected.

V. CONCLUSIONS

A concept of the heterogeneous numerical model of concrete for GPR simulations was presented. After the model validation, a good accuracy with experimental results was revealed. Replacing the dispersion properties of water using the conductivity led to the expected reduction in the amplitude of signal reflections. Numerical GPR simulations conducted on the real structure with a high degree of concrete saturation showed the advantage of the heterogeneous numerical model of concrete over the homogeneous model. Further studies will be directed to verify the reliability of the proposed model by conducting experimental investigations.

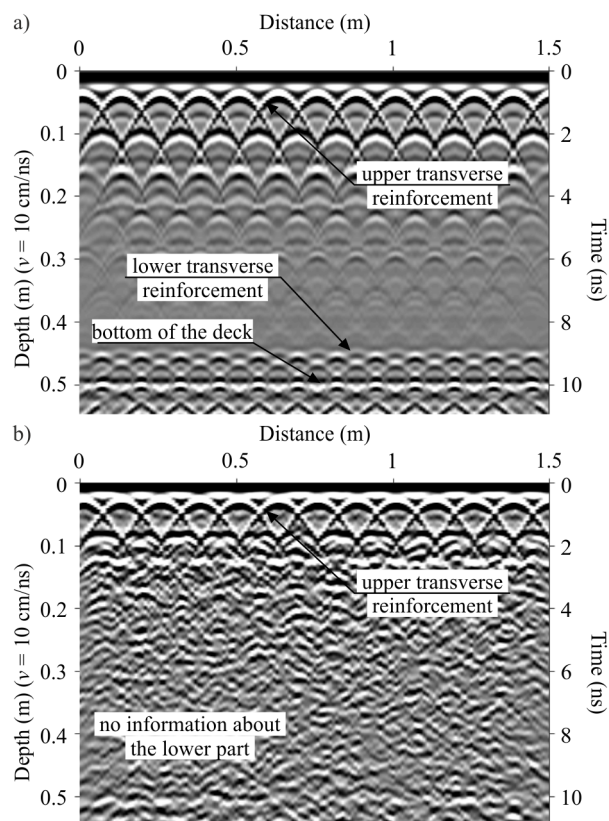


Fig. 8. Numerical GPR maps for a) homogenous and b) heterogeneous models of concrete

REFERENCES

- [1] N. R. Peplinski, F. T. Ulaby, and M. C. Dobson, "Dielectric Properties of Soils in the 0.3–1.3-GHz Range," *IEEE Trans. Geosci. Remote Sens.*, vol. 33, no. 3, pp. 803–807, 1995.
- [2] I. Giannakis, A. Giannopoulos, and C. Warren, "A Realistic FDTD Numerical Modeling Framework of Ground Penetrating Radar for Landmine Detection," *IEEE J. Sel. Top. Appl. Earth Obs. Remote Sens.*, vol. 9, no. 1, pp. 1–15, 2015.
- [3] A. Robert, "Dielectric permittivity of concrete between 50 Mhz and 1 Ghz and GPR measurements for building materials evaluation," *J. Appl. Geophys.*, vol. 40, pp. 89–94, 1998.
- [4] X. Xiao, A. Ihamouten, G. Villain, and X. Dérobert, "Parametric study on processing GPR signals to get a dispersion curve," *Proc. 15th Int. Conf. Gr. Penetrating Radar, GPR 2014*, pp. 575–580, 2014.
- [5] S. Laurens, J. P. Balyssac, J. Rhazi, G. Klysz, and G. Arliguie, "Non-destructive evaluation of concrete moisture by GPR: experimental study and direct modeling," *Mater. Struct.*, vol. 38, no. 283, pp. 827–832, 2005.
- [6] M. Rucka, J. Lachowicz, and M. Zielińska, "GPR investigation of the strengthening system of a historic masonry tower," *J. Appl. Geophys.*, vol. 131, no. 131, pp. 94–102, 2016.
- [7] C. Warren, A. Giannopoulos, and I. Giannakis, "gprMax: Open source software to simulate electromagnetic wave propagation for Ground Penetrating Radar," *Comput. Phys. Commun.*, vol. 209, pp. 163–170, 2016.
- [8] R. Luebbers, F. P. Hunsberger, K. S. Kunz, R. B. Standler, and M. Schneider, "A frequency-dependent finite-difference time-domain formulation for dispersive materials," *IEEE Trans. Electromagn. Compat.*, vol. 32, no. 3, pp. 222–227, 1990.